FTIR study of ageing of γ-irradiated biopharmaceutical EVA based film

Fanny Gaston [a, b, d], Nathalie Dupuy [a, *], Sylvain R.A. Marque [b, c, **], Magali Barbaroux [d], Samuel Dorey [d]

[a] Aix Marseille Univ, CNRS, IRD, Avignon Université, IMBE UMR 7263, 13397, Marseille, France
[b] Aix Marseille Univ, CNRS, ICR, case 551, 13397 Marseille cedex 20, France
[c] Vorozhtsov Novosibirsk Institute of Organic Chemistry Office 312, 9 Prospect Academician Laurentiev, 630090 Novosibirsk, Russia
[d] Sartorius Stedim FMT S.A.S, Z.I. Les Paluds, Avenue de Jouques CS91051, 13781 Aubagne Cedex, France

ARTICLE INFO

ABSTRACT

In the biopharmaceutical and biotechnological industries, disposable plastic bags are used to replace stainless steel vessels. A single-use bag is made up of a film, very often a multilayer structure, which provides good sealability of the contact layer, robustness and barrier to gas. Ethylene vinyl acetate (EVA) is one of the materials constitutive of this multilayer structure. Because these single-use plastic bags have to be sterile upon delivery, they are irradiated at doses between 25 and 45 kGy. The present work aims to investigate the effects of γ-irradiation on the surface of the multilayer film by Fourier Transform Infrared (FTIR) spectroscopy. Optical spectroscopy techniques are of great interest for chemical analysis and are used to obtain information on the composition of materials, in our present case polymers. The chemical changes are monitored over time (up to 12 months) after γ-irradiation (up to 270 kGy) using FTIR to study the composition and stability of the film. The chemometric method called Principal Component Analysis (PCA) is used to highlight the changes in shift or intensity in the oxidation zone and in the unsaturated group zone.

1. Introduction

Single-use plastic bags are more and more frequently applied within the biopharmaceutical and biotechnological industries. Single-use plastic bags in particular are used to replace stainless steel vessels to store and to transport various solutions. The difficult cleaning of the vessel is thus avoided and the possible cross-contamination between two successive uses of the vessel is eliminated. A small upfront capital outlay and a rapidly deployed manufacturing capacity are two other assets of this single-use technology [1]. Most of the bags are provided sterile to the end-users by γ-irradiation, which is the most preferred amongst the sterilization techniques on the biopharmaceutical market today. One of the key properties expected from the single-use bag is the ability to maintain the biocompatibility of the stored solution until

the final application. Therefore all interactions between the material the bag is made of and the solution have to be carefully studied. The material is a multilayer film of ethylene vinyl acetate (EVA) and polyethylene-co-vinyl alcohol (EVOH): EVA/EVOH/EVA. These polymers are selected for their flexibility and barrier properties [2]: polyethylene and EVA are barrier to water and EVOH is barrier to CO_2 and O_2 molecules. It is known that γ-sterilization of EVA polymer leads to alterations of the material: changes in the additives or potential damage to the polymer [3—7]. The present study focuses on the impact of γ-irradiation on the surface of the EVA based film. Although the conventional γ-irradiation dose range used for the biopharmaceutical industry is between 25 and 45 kGy [8], the γ-irradiation doses investigated in this study are up to 270 kGy in order to emphasize the effect of the γ-irradiation and therefore to investigate thoroughly the modifications induced. In our study, as well as the γ-irradiation induced ageing, (quickly visible on the film surface), natural ageing (resulting in slight changes in the polymer structure) is also investigated [9,10]. The irradiation process also leads to the production of radicals, which can generate changes in the polymer structure. In this work, a spectroscopic study on natural ageing after γ-irradiation is performed during one year. The alterations generated on the film

* Corresponding author. Aix Marseille Université, LISA, EA4672, Equipe METICA, 13397 Marseille Cedex 20, France.
** Corresponding author. Aix Marseille Université, Institut de Chimie Radical-aire—UMR 7273, Case 551, 13397 Marseille cedex 20, France.
E-mail addresses: nathalie.dupuy@univ-amu.fr (N. Dupuy), sylvain.marque@univ-amu.fr (S.R.A. Marque).

surface are monitored by ATR-FTIR (Attenuated Total Reflectance − Fourier Transform Infrared) spectroscopy. FTIR spectra are recorded and sampled during up to 12 months, to check composition and stability over time. Variations in FTIR spectra recorded after the γ-irradiation stage are enhanced using the chemometric PCA (Principal Component Analysis) method. PCA makes it possible to focus on different zones of the spectrum to highlight the minor variations, which might be considered as noise. Some degradation mechanisms are proposed in order to describe the changes observed in FTIR spectra. The γ-irradiation induces modifications of the molecular structure: introduction of oxygen in the carbon chain, cross-linking and chain scission.

2. Materials and methods

2.1. Film sample

The film is composed of 2 layers of ethylene vinyl acetate (EVA − 18% vinyl acetate) and one layer of ethylene vinyl alcohol (EVOH), and has a total thickness of about 360 μm. The structure of the entire film, as well as those of the EVA and EVOH polymers is depicted in Fig. 1. The different layers of this film contain additives including at least one antioxidant (especially phenol and phosphite [11–13]). Film samples contain additives for their stabilization during the manufacturing process and during their shelf life. Only the internal layer (contact layer), which will be in contact with the solution in the future applications, was investigated. Moreover, recordings were performed up to 12 months after γ-irradiation. Natural ageing was studied during 0, 1, 2, 3, 4, 6, 12 months (T0, T1m, T2m, T3m, T4m, T6m, T12 m). The measurements were performed on six batches. As they all afford the same observations, only one batch will be discussed hereafter. The samples were stored according to customer requirements: not exposed to direct light and in a room with temperature around 27 ± 5 °C.

2.2. γ-irradiation

Sheets of film (thickness of about 360 μm) were packed and wrapped in specific packaging (polyethylene, PE) and irradiated at room temperature using a ^{60}Co γ-source. This ^{60}Co γ-source provides a dose rate of 8–13 kGy/h − as given by Synergy Health Marseille, France − affording doses of 30 (±1), 50 (±1), 115 (±2) and 270 (±5) kGy. A sterilization cycle corresponds approximately to 30 kGy. To obtain the expected dose, it is necessary to perform several sterilization cycles, including a non-controlled waiting time between each cycle and under non-controlled storage conditions. The samples were analyzed for the first time about 10 days after γ-irradiation.

Concerning the impact of the γ-dose on the polymer, we assume that what happens at high doses, occurs less obvious way to low doses.
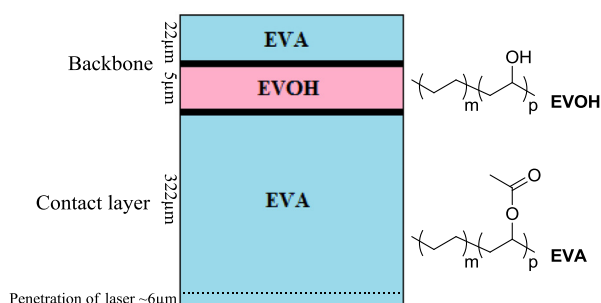

Fig. 1. Structure of film.

2.3. Fourier transform infrared spectroscopy (FTIR)

Film samples were deposited without preparation on the Bruker "Golden Gate" attenuated total reflectance accessory equipped with a diamond crystal. ATR-FTIR spectra of film samples were recorded from 4000 to 650 cm^{-1} (field of mid-infrared), with 4 cm^{-1} resolution and 64 scans using a Thermo Nicolet Avatar spectrometer equipped with a MCT/A detector, an Ever-Glo source, and a KBr/germanium beam splitter. The MIR (Mid-Infrared) spectrometer was installed in an air-conditioned room (21 °C). Three or five spectra were recorded for each sample to reduce the possible effect of film inhomogeneity. A background scan in air (under the same resolution and scanning conditions as those used for the samples) was carried out before three or five sets of acquisition. The ATR crystal was carefully cleaned with ethanol to remove any residual traces of the previous sample. Cleanliness was checked by recording a background spectrum. The penetration depth in the sample is only a few microns [14].

2.4. Principal component analysis

Principal Component Analysis (PCA) [15] is a method used to extract the systematic variations from a data set. PCA reduces the dimensionality of data with a minimum loss of information. The main systematic variation in the data set is given by the principal component, PC. The common characteristics of all spectra are modeled in one or several PC. Plotting two PCs relatively to each other affords an analysis of the interaction between two PCs, thanks to the similarities or differences between samples [16,17]. In matrix representation, the model with a given number of components has the following equation:

$$X = T \cdot P^T + E$$

where T is the scores matrix, P the loadings matrix and E the error matrix. The PCA were performed with Unscrambler software.

The impact of γ-irradiation on the internal EVA layer was investigated by PCA. We investigated the variations in intensity and shift of the FTIR peaks (1714 cm^{-1} and 960 cm^{-1}) depending on the irradiation doses. For all PCAs, the EVA spectra were adjusted using the baseline correction (offset correction) tool and/or the smoothing Savitzky Golay algorithm and/or maximum normalization.

3. Results

3.1. ATR-FTIR

The effect of the γ-irradiation doses from 0 (non-sterilized material) to 270 kGy is displayed in Fig. 2. The main changes in signal are observed in the carboxylic acid zone (around 1714 cm^{-1}) and in the *trans* alkene zone (around 960 cm^{-1}). Enlargements of these zones show a variation depending on the γ-dose (Fig. 2), which is emphasized by the PCA. The peaks present in the 730–700 cm^{-1} zone and in the 2920–2840 cm^{-1} zone do not show any variation as a function of the irradiation. In ATR mode, the depth of penetration of the infrared beam into the material is very shallow in the zone around 3000 cm^{-1}, thus slight γ-irradiation induced variations do not result in significant spectral changes. Consequently, cross-linking and chain scission processes are not significant.

The IR assignments of the non-irradiated and irradiated EVA are provided in Table 1 according to the literature [18–27]. Peaks at 2916 and 2848 cm^{-1} correspond to the antisymmetric and symmetric stretching of −CH$_2$− groups. Peaks included between 1470 and 1360 cm^{-1} correspond to the deformation of −CH$_2$− and
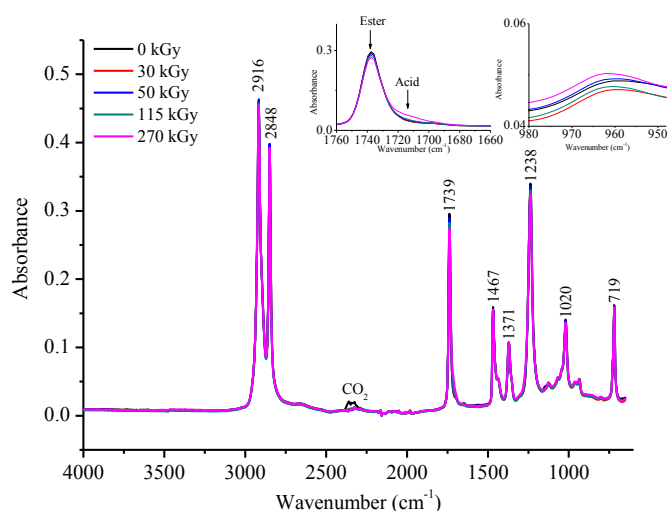
Fig. 2. Overlay of EVA spectra for not sterilized and γ-irradiated samples. Inset: enlargements of the carbonyl zone (left) and of the *trans* alkene zone (right).

−CH₃− groups. Peaks at 720−730 cm^{-1} are characteristic of long chains of −CH₂− present in PE. Peaks at 1739, 1238 and 1020 cm^{-1} characterize the vinyl acetate moiety.

3.2. PCA

In the ATR-FTIR spectra, only two zones (carboxylic acids, [1760−1660/1280−1180 cm^{-1}], and unsaturated groups, [980−950 cm^{-1}]) exhibit changes in the signal. Outside these two zones, the PCA does not reveal any change due to either the γ-irradiation dose or the natural ageing, which confirms that no significant cross-linking or chain scission processes has occurred.

3.2.1. Carbonyl and ester zone

The PCA displayed in Fig. 3 concerns the carbonyl and ester zone [1760−1670/1280−1180 cm^{-1}]. It is performed on 129 spectra, which represent the effects of all γ-irradiation doses and ageing.

For this zone, EVA spectra are baseline corrected and normalized. At initial time (T0), the effect of the dose on the generation of carboxylic acid is significant for a dose of 50 kGy and striking for doses larger than 115 kGy (see Fig. 1 SI). The first principal component (PC1) represents 74% of the total variance of the modification of spectra, and changes are correlated to the γ-irradiation doses. The impact of the γ-dose on the film is not homogeneous: there is an overlap between the 30 kGy irradiated group, the 50 kGy-irradiated group and the non-irradiated group. The irradiation impact is significant above 115 kGy [28]. When the γ-dose increases, there is a decrease in the intensity of the peak at

1739 cm^{-1} (characteristic of C=O in ester) and an increase in the intensity of the peak at 1714 cm^{-1} (characteristic of C=O in acid). This means that the ester part is degraded to provide carboxylic acid functions. Moreover, when the γ-dose increases, the intensity of the peak at 1235 cm^{-1}, characteristic of C−O in ester, decreases (as that of the 1739 cm^{-1} peak) and the intensity of the peak at 1265 cm^{-1} [29], characteristic of C−O in acid, increases (as that of the 1714 cm^{-1} peak). Given the structure of the EVA polymer, it is obvious that acetic acid is released. The increase occurs from 50 kGy and is really significant from 115 kGy. The second component PC2 represents on average 18% of the total variance of the modification of the spectra. For all doses as well for the non-irradiated film, non-regular ageing is observed (Figs. 2 SI−6 SI). Indeed For not-sterilized samples and irradiated samples at 30 and 50 kGy, the formation of carboxylic acid is not clearly detected over time (Figs. 2 SI−4 SI) due to the small amount of acid generated, whereas a clear peak ascribed to the carboxylic function is observed at 115 and 270 kGy (Figs. 5 SI and 6 SI). At 270 kGy, the time impact is clear, however at low doses the time impact is less striking. The gap observed between T2m and T3m is nicely highlighted in Fig. 3b), which displays all doses combined with all ageings. This gap suggests that another reaction occurs after 2−3 months, depending on the doses and on the storage conditions. Indeed, γ-irradiation generates carboxylic acid functions, likely acetic acids, affording an environment that fosters the hydrolysis of the ester functions in the presence of water. However, the presence of the PE copolymer in the EVA layer dramatically slows down the hydration of the material. Then, the amount of water from air moisture required for acid-catalyzed ester hydrolysis is obtained after 3 months of ageing. The time impact is better pronounced for the sample irradiated at 270 kGy and for the sample irradiated at low γ-doses the time impact is less important. The hydrolysis phenomena are more observable for the high γ-doses, especially for samples irradiated at 270 kGy.

3.2.2. Unsaturation zone

The PCA displayed in Fig. 4 concerns the unsaturated group zone between 980 and 950 cm^{-1}. It is performed on 129 spectra, which represent the effects of all γ-irradiation doses and ageing.

For this zone, the EVA spectra are baseline corrected. The first principal component (PC1) represents 97% of the total variance of the modification of the spectra, and corresponds to the γ-irradiation doses. In this zone, the impact of the irradiation is visible from 30 kGy. Indeed the bar height for 30, 50, 115 and 270 kGy irradiated samples decreases significantly compared to those for non-sterile samples. The PCA results show that the intensity of the peak at 964 cm^{-1} (−R₁−CH=CH−R₂, *trans* vinylene group) increases when the γ-dose increases, meaning modifications occur in the EVA chains [6,24,30,31] (vide infra). The second principal component (PC2) represents only 3% of the total variance of the modification of the spectra and does not merit further comment. The variance of

Table 1
IR assignments of bands for PE spectra.

Wavenumber (cm^{-1})	Functional group	Type of vibration
2916	ν−CH₂−	Antisymmetric stretching [19,20]
2848	ν−CH₂−	Symmetric stretching [19,20]
1739	ν−C=O ester	Stretching [18,24]
1714	ν−C=O carboxylic acid	Stretching [23,25,26]
1467−1438	δ−CH₂−	Deformation in the plane [19,20,24]
1371	δ CH₃	Deformation in the plane [19,20,24]
1300−1020	ν−C−O	Stretching [24,25]
964	−R₁−CH=CH−R₂	*Trans* vinylene group [21,22]
730 (shoulder)	δ−CH₂−	Inner rocking vibration of −CH₂− in the crystalline part [24,27]
717	δ−CH₂−	Inner rocking vibration of −CH₂− in the amorphous part [24,27]
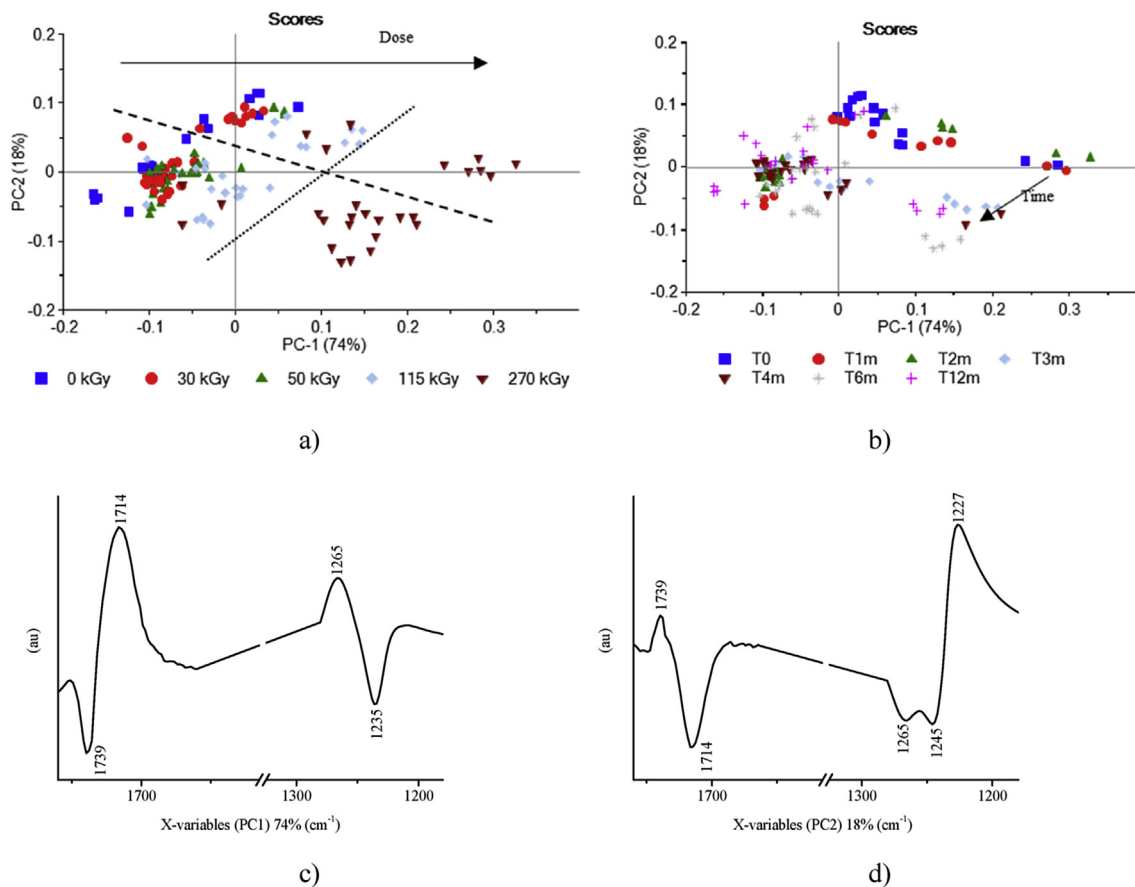
Fig. 3. PCA of EVA spectra at all γ-irradiation doses (1760—1670/1280—1180 cm^{-1}). Spectra are baseline corrected and normalized. a) Score plot of PCA with γ-dose labels. Dashed line delimits the ageing groups and dotted line delimits the γ-doses groups. b) Score plot of PCA with time labels. c) Loading plot of PC1. d) Loading plot of PC2.

this component is due to the uncertainty in the measurements and cannot be ascribed to the natural ageing.

4. Discussion

The 30 kGy γ-dose is obtained after a passage of about 3 h in front of the 60Co source, the 50 kGy γ-dose is obtained after about 6 h, and so on. As observed with the PCA displayed in Fig. 3 a, the differences between 0, 30 and 50 kGy groups are small, so it is difficult to discuss about the chemistry in these cases. Therefore, for

the discussion, 115 and 270 kGy γ-doses are assumed to enhance the chemical processes occurring at lower doses. This assumption is supported by the absence of new rising signals in the FTIR spectra when γ-doses are increased from 50 to 115 and 270 kGy.

The results reported above − generation of carboxylic acid combined with degradation of ester, and formation of *trans* C=C − are described by several mechanisms. The C=O and C−O−C groups have the lower ionization potential (IP), $IP_{(C-O-\overset{+}{C})} = 9.70$ eV, $IP_{(CH)}^{+} = 10.70$ eV, $IP_{(C=\overset{+}{O})} = 10.94$ eV, $IP_{(C-\overset{+}{C})} \sim 11.20$ eV [32]. Therefore, it is likely that the radical species will be generated from
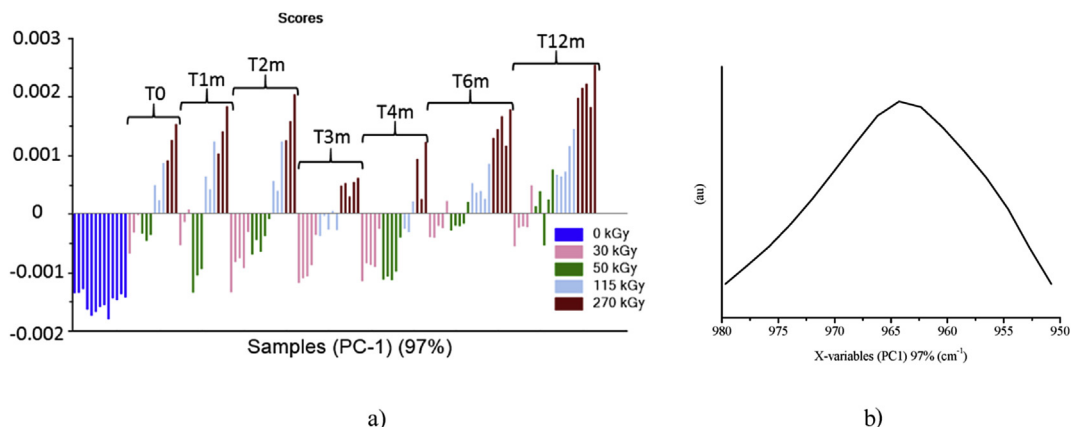
Fig. 4. PCA of EVA spectra at all γ-irradiation doses (980—950 cm^{-1}). Spectra are baseline corrected. a) Score plot of PCA. b) Loading plot of PC1.
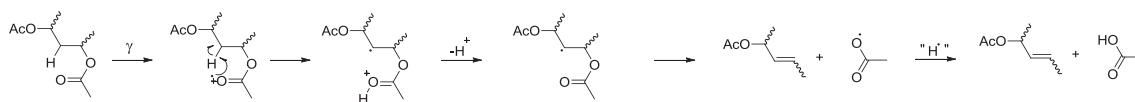
Scheme 1. Radical pathway for the formation of acetic acid.

these groups. Only the acetate function is considered to account for the formation of carboxylic acid. Indeed the formation of a radical cation is more probable on the vinyl acetate moiety than on the polyethylene moiety.

Carboxylic acids are generated in two stages. During the first two months after γ-irradiation, and after the 3rd month the hydrolysis increases the amount of carboxylic acids until 6 months. Consequently, such results are ascribed to two different processes: one relying on radical chemistry due to the γ-irradiation, and a second one relying on the ionic hydrolysis due to the natural ageing of material.

Under γ-irradiation, a radical cation is likely generated on the carbonyl function (Scheme 1). A 1,5-hydrogen atom transfer is expected to afford an alkyl radical at position β to the O-atom of the ester bond. Then, β-fragmentation occurs, affording an alkene (for discussion vide infra) and an acetyloxyl radical which can readily abstract an H-atom to afford a carboxylic acid. 1,4-H and 1,6-H transfers are disregarded as they should generate an acetoxyalkyl radical, very similar to a hydroxyalkyl radical, which should be revealed by electron spin resonance, as is observed for irradiated EVOH [33].

Under γ-irradiation, the generation of the radical cation B on the ester oxygen may be also expected (Scheme 2). A 1,5-hydrogen atom transfer can occur, providing an alkyl radical and an oxonium ion C. The latter collapses to release acetic acid and a carbocation D. Then a 1,3 shift of the acetoxy group occurs through a cyclic carbocation E followed by β-fragmentation of the alkyl radical to generate an oxyl radical with a carbocation in α-position F. The oxyl radical readily abstracts an H-atom to generate an α-dioxygenated cation which releases a proton to provide an ester function. The released proton can play the role of the catalyst for the hydrolysis of the ester function in the presence of traces of water. On the other hand, the alkyl radical C is in the β position to the ester function and then prone to β-fragmentation to generate an acetyloxyl radical, as described in Scheme 1. These two schemes account for the large generation of acetic acid during γ-irradiation, and for the amount of acetic acid observed during the first two months of ageing (Fig. 3). 1,4-H and 1,6-H transfers are disregarded

as they should generate an acetoxyalkyl radical, very similar to a hydroxyalkyl radical which should be revealed by electron spin resonance, as observed for irradiated EVOH [33].

Then, after 3 months, the presence of acetic acids induces the catalysis of the hydrolysis of the ester by water [34] (Scheme 3), especially for samples irradiated at 270 kGy. Assuming that acetic acid migrates more slowly than water, upon ageing water from air can cross the PE copolymer in the EVA layer to reach the vinyl acetate layer. This phenomenon is not clearly highlighted for the low doses, as shown by individual PCA in Figs. 2—5 SI.

The formation of *trans* alkene is due to either two fragmentation reactions or to H-abstraction. In Scheme 1, the β-fragmentation generates an alkene along with the carboxylic acid. During γ-irradiation, several highly reactive radicals are generated, such as acetoxyl radical which are prone to abstract an H-atom which can be either in 5th position to the O-atom of the ester bond (Scheme 2) or in α position to the O-atom of the ester bond (Scheme 4).

As described in Scheme 4, the formation of the *trans* alkene is favored, as it exhibits the lowest steric hindrance The formation of double bonds is due to the abstraction of the H-atom (route A) and to two fragmentation processes (route B and route C). The Bond Dissociation Energies (BDE) of some model radicals are about 128 kJ mol^{-1} [35] for the abstraction of the H-atom in β-position, about 121 kJ mol^{-1} [36] for the β-fragmentation of the hydroxyl group, and about 91 kJ mol^{-1} [37] for the β-fragmentation in alkyl radicals. Taking into account that route B leads to the formation of an acyloxyl radical with an odd electron stabilized by conjugation with the C=O bond, the BDE corresponding to route B is expected to be lower than 121 kJ mol^{-1} and route B the likely favored process.

For reasons of steric hindrance, the *trans* configuration is preferably adopted. As shown in Scheme 4, whatever the reaction, the radical has to adopt the less hindered conformation affording the *trans* isomer. The H-abstraction and the C—C bond fragmentation afford an enol ester as alkene. Thus, the hydrolysis of this enol ester (Scheme 5) into enol and acetic acid is likely due to the presence of γ-irradiation generated acetic acid and water (vide supra). This enol tautomerizes spontaneously into ketone.
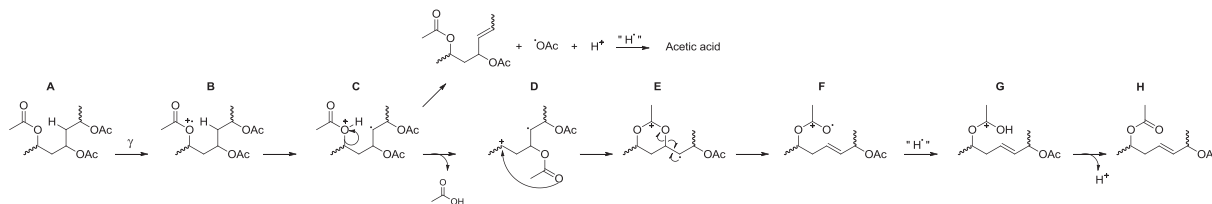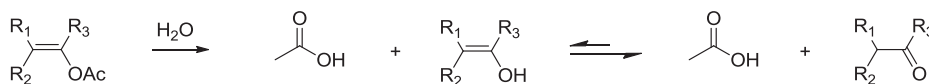

Scheme 2. Radical manifold for the formation of acetic acid.
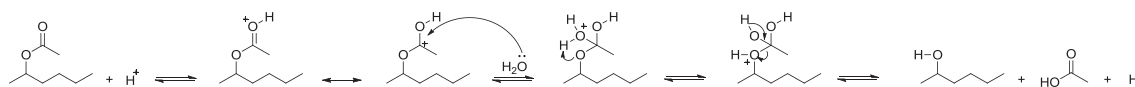
Scheme 3. Hydrolysis of ethylene vinyl acetate.
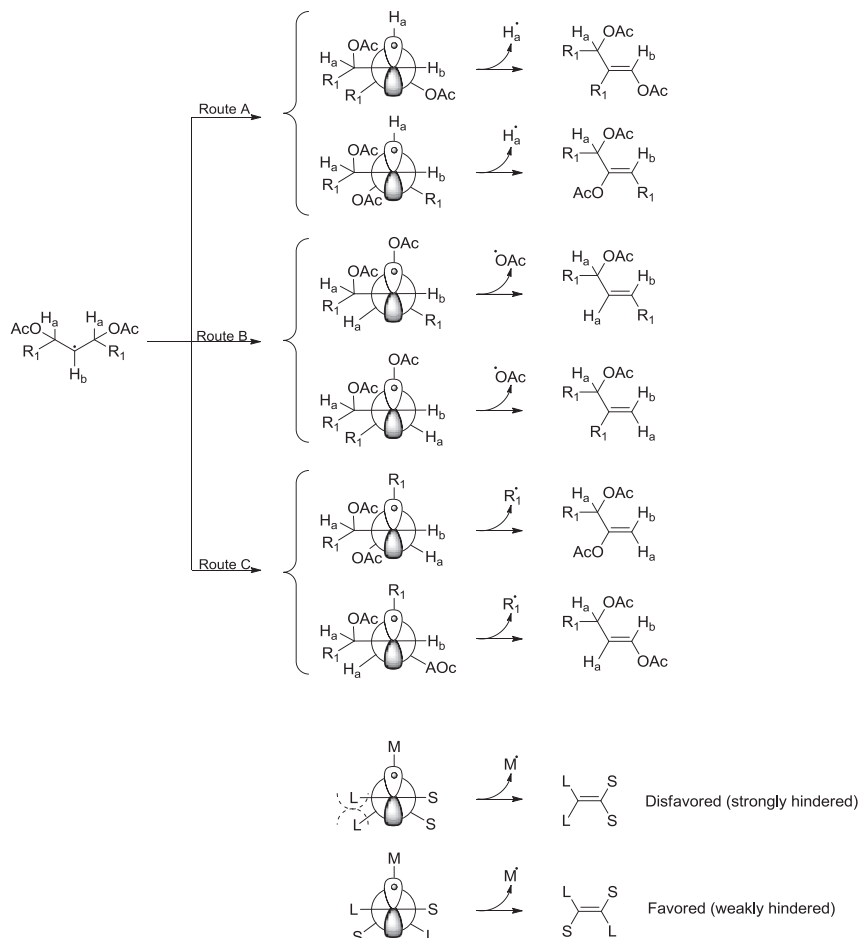
Scheme 4. Radical pathway for the formation of the *trans* alkene. L: large group; M: medium group; S: small group.

Scheme 5. Hydrolysis of vinyl acetate derivative.

5. Conclusion

In this study, FTIR spectroscopy is used to monitor the impact on an EVA based multilayer film of γ-irradiation at different doses (0, 30, 50, 115 and 270 kGy) and over time. The results observed on an EVA based multilayer film are in good agreement with literature data [5,21—25]. The PCA method is used to highlight unambiguously the formation of carboxylic acids with characteristic stretching vibrations: ν C=O (1714 cm^{-1}) and ν C—O (1265 cm^{-1}). It emphasizes minor alterations to the material. On the PE copolymer of EVA no significant changes are observed, meaning only weak alterations occur under γ-irradiation: low oxidation, low chain fragmentation and low cross-linking on the film surface. This method highlights two different ageing processes: the γ-ageing and the natural ageing, the latter having practically no impact. To take into account these PCA results, the well-known mechanisms in the literature are used. During irradiation, radical species are formed along with other organic functions, leading to the formation of carboxylic acids and unsaturated groups. The carboxylic acids and unsaturated groups are observed on the film surface in this study, but it is probable that these compounds are also present in the core of the EVA layer, in correlation with O_2 migration through the film. The formation of carboxylic acid can result from γ-irradiation or from natural ageing (hydrolysis). The absence of carboxylic acid in a sample subjected to neither irradiation nor ageing (at 0 kGy and T0) means that carboxylic acid cannot be generated during the film manufacturing process.

Acknowledgements

Appendix A. Supplementary data

Supplementary data related to this article can be found at http://dx.doi.org/10.1016/j.polymdegradstab.2016.03.040.

References

[1] C.H. Arnaud, Disposable plastic bioreactors lead to savings—and challenges—for biopharma firms, Chem. Eng. News 93 (2015) 10—13.

[2] A.E. Goulas, K.A. Riganakos, M.G. Kontominas, Effect of ionizing radiation on physicochemical and mechanical properties of commercial multilayer coextruded flexible plastics packaging materials, Radiat. Phys. Chem. 68 (2003) 865—872.

[3] K.J. Hemmerich, Medical Device and Diagnostic Industry, 2000 online: http://www.mddionline.com/article/polymer-materials-selection-radiation-sterilized-products.

[4] N.H. Stoffers, J.P.H. Linssen, R. Franz, F. Welle, Migration and sensory evaluation of irradiated polymers, Radiat. Phys. Chem. 71 (2004) 203—206.

[5] M. Sen, M. Copuroglu, A comparative study of gamma irradiation of poly(ethylene-co-vinyl acetate) and poly(ethylene-co-vinyl acetate)/carbon black mixture, Mater. Chem. Phys. 93 (2005) 154—158.

[6] S.K. Dutta, A.K. Bhowmick, P.G. Mukunda, T.K. Chaki, Thermal degradation studies of electron beam cured ethylene-vinyl acetate copolymer, Polym. Degrad. Stabil. 50 (1995) 75—82.

[7] P.G. Demertzis, R. Franz, F. Welle, The effects of γ-irradiation on compositional changes in plastic packaging films, Packag. Technol. Sci. 12 (1999) 119—130.

[8] Guide to Irradiation and Sterilization Validation of Single-use Bioprocess Systems, Bioprocess International, May 2008, p. 12.

[9] A. Rjeb, L. Tajounte, M. Chafik el Idrissi, S. Letarte, A. Adnot, D. Roy, Y. Claire, A. Périchaud, J. Kaloustian, IR spectroscopy study of polypropylene natural aging, J. Appl. Polym. Sci. 77 (2000) 1742—1748.

[10] B. Youssef, A. Elkader Dehbi, A. Hamou, J.-M. Saiter, Natural ageing of tri-layer polyethylene film: evolution of properties and lifetime in North Africa region, Mater. Des. 29 (2008) 2017—2022.

[11] D.H. Jeon, G.Y. Park, I.S. Kwak, K.H. Lee, H.J. Park, Antioxidants and their migration into food simulants on irradiated LLDPE film, LWT 40 (2007) 151—156.

[12] F. Bourges, G. Bureau, J. Dumonceau, B. Pascat, Effects of electron beam irradiation on antioxidants in commercial polyolefins: determination and quantification of products formed, Packag. Technol. Sci. 5 (1992) 205—209.

[13] J. Pospisil, Chemical and photochemical behaviour of phenolic antioxidants in polymer stabilization-a state of the art report, Part I, Polym. Degrad. Stabil. 40 (1993) 217—232.

[14] Harrick formula gives the depth penetration corresponding to a given wavenumber: $dp = \lambda / \sqrt{2\pi n1 \left(\sin^2 \theta - \left(\frac{n2}{n1} \right)^2 \right)}$ with dp, the depth penetration; λ, the given waven. umber; n_1, refractive index of sample (n_1=1.5 for the majority of organic materials, P. Liu et alEnviron. Sci. Technol. 47 (2013) 13594-13601; J-G Liu, et al. J. Mater. Chem. 19(2009) 8907—8919); n_2, refractive index of diamond crystal (n_2=2.417); θ, angle of incidence of the beam relative to the normal of the diamond interior (θ=45°). Depth penetration is around 6 μm for λ=700 cm^{-1}, and around 0.3 μm for λ=4000 cm^{-1}.

[15] H. Martens, T. Naes, Multivariate Calibration, Wiley, 1989.

[16] N. Kumar, A. Bansal, G.S. Sarma, R.K. Rawal, Chemometrics tools used in analytical chemistry: an overview, Talanta 123 (2014) 186—199.

[17] K.H. Esbensen, D. Guyot, F. Westad, L.P. Houmoller, Multivariate Data Analysis: in Practice: an Introduction to Multivariate Data Analysis and Experimental Design, 2002.

[18] G. Socrates, Infrared and Raman Characteristic Group Frequencies, third ed.,

[19] R.P. Wool, R.S. Bretzlaff, Infrared and Raman spectroscopy of stressed polyethylene, J. Polym. Sci. Pol. Phys. 24 (1986) 1039—1066.

[20] G. Socrates, Infrared and Raman Characteristic Group Frequencies, third ed., 2004, p. 268.

[21] L.H. Cross, R.B. Richards, H.A. Willis, The infra-red spectrum of ethylene polymers, Discuss. Faraday Soc. 9 (1950) 235—245.

[22] F.J. Boerio, S. Wirasate, in: Neil J. Everall, John M. Chalmers, Peter R. Griffiths (Eds.), Measurements of the Chemical Characteristics of Polymers and Rubbers by Vibrational Spectroscopy, in Vibrational Spectroscopy of Polymers: Principles and Practice, John Wiley and Sons, 2007, p. 114.

[23] J. Lacoste, D.J. Carlsson, Gamma-, photo-, and thermally-initiated oxidation of linear low density polyethylene: a quantitative comparison of oxidation products, J. Polym. Sci. Pol. Chem. 30 (1992) 493—500.

[24] M. Giurginca, L. Popa, T. Zaharescu, Thermo-oxidative degradation and radioprocessing of ethylene vinyl acetate elastomers, Polym. Degrad. Stabil. 82 (2003) 463—466.

[25] G. Socrates, Infrared and Raman Characteristic Group Frequencies, third ed., 2004, p. 125.

[26] Z. Liu, S. Chen, J. Zhang, Photodegradation of ethyleneeoctene copolymers with different octene contents, Polym. Degrad. Stabil. 96 (2011) 1961—1972.

[27] D. Klepac, M. Scetar, G. Baranovic, K. Galic, S. Valic, Influence of high doses γ-irradiation on oxygen permeabilityof linear low-density polyethylene and cast polypropylene films, Radiat. Phys. Chem. 97 (2014) 304—312.

[28] For the samples irradiated at 270 kGy, we observe 6 outliers, with no rational at this time.

[29] In some articles [5,24], the peak at 1714 cm^{-1} is attributed to the ketone function. It is possible that the authors had actually observed an acid carboxylic function, because they did not notice the peak variations at 1265 cm^{-1} characterizing the stretching C—O in a carboxylic acid, which are observed here thanks to PCA.

[30] F. Khodkar, N.G. Ebrahimi, Effect of irradiation on mechanical and structural properties of ethylene vinyl acetate copolymers hollow fibers, J. Appl. Polym. Sci. 119 (2011) 2085—2092.

[31] J. Jin, S. Chen, J. Zhang, UV aging behaviour of ethylene-vinyl acetate copolymers (EVA) with different vinyl acetate contents, Polym. Degrad. Stabil. 95 (2010) 725—732.

[32] R.D. Levin, S.G. Lias, Ionization potential and appearance potential measurements, 1971-1981.

[33] G. Audran, S. Dorey, N. Dupuy, F. Gaston, S.R.A. Marque, Degradation of γ-irradiated polyethylene-ethylene vinyl alcohol-polyethylene multilayer films: an ESR study, Polym. Degrad. Stabil. 122 (2015) 169—179.

[34] The lack of alcohol fingerprints (ν-OH 3300 cm^{-1}, ν-C-O 1200—1000 cm^{-1}) is due to:i) low concentration in alcohol as it is generated only by hydrolysis (Scheme 2); ii) The ν-OH stretching corresponds to the wideband and is therefore weakly noticeable; iii) The zone corresponding to the ν-C-O stretching in the alcohol can be included under the ν-C-O stretching in the carboxylic acid.

[35] Yu-Ran Luo, Comprehensive Handbook of Chemical Bond Energies, 2007, p. 143. BDE for $CH_3C \cdot HCH_2OH$.

[36] Yu-Ran Luo, Comprehensive Handbook of Chemical Bond Energies, 2007, p. 346. BDE for CH3CH2CH2CH2-CH2C·HCH3.

[37] Yu-Ran Luo, Comprehensive Handbook of Chemical Bond Energies, 2007, p. 208. BDE for OH-CH(CH3)C·H2.